Article

INTERNATIONAL JOURNAL OF DAMAGE MECHANICS

Strength reduction method for a factor of safety determination of damaged concrete structures

International Journal of Damage Mechanics
0(0) 1–19

DOI: 10.1177/10567895231183469
journals.sagepub.com/home/ijd
Sage

Dragan Rakić[1], Vladimir Dunić[1], Miroslav Živković[1], Slobodan Radovanović[2], Dejan Divac[2] and Dragoslav Šumarac[3]

Abstract

The paper presents the procedure for determining the factor of safety (FoS) using the strength reduction method (SRM) for the case of a concrete damage plasticity constitutive model. The SRM was originally used in a slope stability analysis and in its original form, this method was applied by reducing the shear strength of the material. Since damage in concrete occurs due to exceeding the normal stresses in the principal directions, and not due to exceeding the shear strength, this method was modified and adapted to the concrete damage plasticity constitutive model. Instead of reducing the failure surface, the parameters which describe the mechanical behavior in the case of uniaxial compression and uniaxial tension were reduced. In this way, the reduction of stress and the corresponding strain was carried out in the entire range of total strain, without changing the shape of the failure surface in the deviator plane. For the proposed methodology, a numerical algorithm was developed and implemented into the software PAK. The algorithm was verified through test examples and the obtained results were compared with analytically calculated FoS. The excellent agreement is observed between the FoS obtained by applying the proposed algorithm and the analytically calculated FoS.

Keywords

Factor of safety, strength reduction method, concrete damage plasticity model, finite element method, PAK software

Introduction

Engineering (civil and mechanical) structures are involved in the essential segments of people's lives, so safety is the most important demand in a structural design. For quantitative safety expression, a Factor of Safety (FoS) can be defined as (1) the maximum load-bearing capacity of a structure or

[1]University of Kragujevac, Faculty of Engineering, Kragujevac, Serbia
[2]Jaroslav Černi Water Institute, Belgrade, Serbia
[3]State University of Novi Pazar, Department of Technical Sciences, Novi Pazar, Serbia

Corresponding author:
Dragan Rakić, University of Kragujevac, Faculty of Engineering, Sestre Janjić 6, Kragujevac 34000, Serbia.
Email: drakic@kg.ac.rs

(2) the safety margin for a structure according to recommendations or requirements. Also, the structure FoS can be defined as the ratio of the strength of the material to the minimum strength necessary to prevent failure. Different industries provide different FoS requirements. If the consequences of the potential failure are more significant, a higher margin will be required. So, the questions related to the procedures for FoS determining are open and the engineering community tends to improve them.

Before applying numerical methods, the FoS of geotechnical structures was determined using the Limit Equilibrium Method (LEM) (Bishop, 1955; Janbu, 1954; Spencer, 1967). However, with the increase in computer efficiency, numerical methods have an increasing presence for determining the FoS. In the slope stability analysis using LEM, it is necessary to form vertical sections in the analyzed volume, which requires the introduction of additional assumptions about the directions of interaction forces, which may affect the equilibrium conditions (Griffiths and Lane, 1999).

The fib Model Code considers two approaches possible for assessing the structural safety of concrete structures (Couto et al., 2015): the Probabilistic Method and the Partial Safety Factor Method. In addition, the fib Model Code presents two partial safety factor methods for existing concrete structures as possibilities to determine FoS (Caspeele et al., 2013; Lara et al., 2021): the Design Value Method (DVM) and the Adjusted Partial Factor Method (APFM). The DVM proposes a procedure for evaluating partial factors, while the APFM provides factors for new structures. Unfortunately, these methods do not give reliable results for concrete structures because of sensitivity to a change of failure mechanism. Furthermore, these models can lead to unreliable design when loading and boundary conditions are more complex, which can be assessed only using non-linear FEM simulation (Abra and Ben Ftima, 2020). Advanced non-linear FE can be used to solve complex design problems, but is rarely used in engineering practice. In (Woliński, 2011), Woliński investigated global safety factors using nonlinear concrete structure analysis. He compared several practical methods by using nonlinear analysis. Firstly, he presented linear and nonlinear analysis using Eurocodes in partial factors format. Further, the global factor format for nonlinear analysis is considered, such as the ECOV method (Estimate of Coefficient of Variation) (Lara et al., 2021). In the end, Woliński presented a method that considers two partial coefficients products with the advantage of only one nonlinear simulation.

The application of numerical methods does not require the introduction of assumptions regarding the shape and location of occurrence of sliding surfaces. So, they are more suitable for application in complex engineering problems, because the sliding surface is determined automatically (Cheng et al., 2007; Manzari and Nour, 2000; Zhang and Chen, 2004). Furthermore, various authors have confirmed that the FoS obtained using numerical methods is the same as the FoS obtained using LEM, provided that the appropriate density of the finite element mesh is used (Cheng et al., 2007; Dawson and Roth, 1999; Griffiths and Lane, 1999).

In general, two methods in the numerical analysis (Xue et al., 2018) are used: (1) Overload method – in which the load is increased gradually, while the strength of the material remains unchanged (Li et al., 2009; Sarma, 1973; Seo, 1998), and (2) Strength Reduction Method (SRM) – in which the strength of the material is gradually reduced, while the loading conditions remain unchanged (Dawson and Roth, 1999; Griffiths and Lane, 1999; Naylor, 1982). Both methods gradually bring the analyzed structure to a state of limit equilibrium (the state immediately before the failure). However, by using the overload method to determine the FoS of geotechnical structures, due to different types of loads and directions of their effect, different authors can obtain various safety factors, so this represents a significant drawback of this method (Xue et al., 2018). Many commercial software for numerical analysis of geotechnical structures, based on the

Finite Element Method (FEM), apply the SRM to determine the FoS. The SRM was first proposed by Zienkiewicz (Zienkiewicz et al., 1975), and applied in slope stability analysis and is named the shear strength reduction method. Later, its application was accepted for the stability analysis of other geotechnical structures such as embankment dams, foundations of concrete gravity dams, concrete arch dams, and other objects directly interacting with the ground (Dawson and Roth, 1999; Griffiths and Lane, 1999; Naylor, 1982). However, in case of concrete, one cannot speak about shear strength because the failure in concrete occurs due to exceeding the normal (principal) stresses (Lee, 1996; Lubliner et al., 1989; Omidi and Lotfi, 2010). Still, in this case, it is about the strength of the material in general. Determining the FoS using the SRM is often discussed in the literature and is implemented in Finite Element Method (FEM) software solutions (Bentley Systems International Limited, 2019; Kojić and Drugi 2010; Kojić et al., 2011; Zhao and Zheng, 2002) for constitutive models with a linear failure surface, such as the Mohr-Coulomb or Drucker-Prager constitutive models (Dawson and Roth, 1999; Griffiths and Lane, 1999; Zheng et al., 2009). In the case of constitutive models with a non-linear failure surface, the material parameters corresponding to the reduced failure envelope are determined by curve fitting (Fu and Liao, 2010; Hammah et al., 2005). FoS of the structure using the SRM is determined by gradually reducing the strength of the material using the strength reduction factor (SRF), until failure occurs. The maximum value of SRF at which the structure is stable represents the global FoS. From a numerical point of view, the structure is stable (there is no failure), as long as it is possible to achieve convergence of the numerical solutions. Alternatively, the failure can be defined as the point at which the maximum deformation of the structure exceeds the permissible value. However, this criterion is subjective compared to the convergence criterion, so it is less often used in practice.

In this paper, the authors investigated the possibility of applying the SRM to a constitutive model with damage feature, which is a more complex problem and requires more sophisticated analysis. The Concrete Damage Plasticity (CDP) constitutive model proposed by Lubliner and authors (Kiefer et al., 2018; Lubliner et al., 1989) is used to modeling the mechanical behavior of concrete structures. This constitutive model is implemented into the in-house FEM software PAK (Kojić and Drugi, 2010; Kojić et al., 2011) for structural analysis, developed at the Faculty of Engineering, University of Kragujevac, Serbia. The CDP constitutive model describes mechanical behavior of concrete using the stress-strain dependence in uniaxial compression and uniaxial tension tests. By investigating the stress-strain response of the numerical simulations, one can notice that it is necessary to reduce the stress and the corresponding strain (Rakić et al., 2019, 2021), and to determine new material parameters which define uniaxial tension and uniaxial compression stress-strain dependence. Reducing the strength of the CDP model, which includes damage, gives a unique insight into the application of SRM to the constitutive models with damage feature. The proposed procedure for determining the global FoS by SRM is verified by numerical analysis of uniaxial compression and uniaxial tension tests, as well as the bending test of the concrete beam without reinforcement.

The authors first presented the brief theoretical background of the CDP constitutive model implemented in software PAK. In the same section, the details about SRM are given. In section 3, the numerical implementation of SRM for the CDP model is presented in details with the appropriate scheme for incremental implementation. Finally, in section 4, numerical examples are chosen to cover common tests for this type of material. The obtained results are compared to the analytical values of FoS and excellent agreement is observed. Finally, the main conclusions about the obtained results and procedure are given.

Theoretical background

CDP constitutive model

The CDP constitutive model (Lee, 1996; Lubliner et al., 1989; Park et al., 2022; Voyiadjis et al., 2022) has been widely used for the FE analysis of concrete structures. It is a local damage model where the damage and degradation of the stiffness are computed as an internal local variable. The model has been implemented in various FEM software and in the PAK software (Kojić and Drugi, 2010; Kojić et al., 2011) for structural analysis. The details about the model and theoretical background are available in the literature (Lee, 1996; Lee and Fenves, 1998; Lubliner et al., 1989), but the brief theory of the SRM will also be presented in this paper.

The failure surface of the CDP constitutive model (Lubliner et al., 1989) is described by the Ducker-Prager failure surface:

$$F(\bar{\boldsymbol{\sigma}},\boldsymbol{\kappa}) = \frac{1}{1-\alpha}\left(\alpha\bar{I}_1 + \sqrt{3J_{2D}} + \beta(\boldsymbol{\kappa})\langle\bar{\sigma}_{\max}\rangle\right) - c_c(\boldsymbol{\kappa}) \leq 0 \tag{1}$$

and its interpretation in stress space is shown in Figure 1, where:

$\bar{\boldsymbol{\sigma}}$ - effective stress,

$\boldsymbol{\kappa}$ - damage variables,

$\bar{I}_1 = \mathrm{tr}\bar{\boldsymbol{\sigma}}$ - first stress invariant,

$\bar{\sigma}_{\max}$ - algebraic maximum principal stress,

J_{2D} - second deviatoric stress invariant,

$\alpha = \frac{\sigma_{b0}-\sigma_{c0}}{2\sigma_{b0}-\sigma_{c0}}$ - ratio of uniaxial (σ_{c0}) and biaxial (σ_{b0}) failure stress in compression,

$$\beta(\boldsymbol{\kappa}) = \begin{cases} \dfrac{\bar{\sigma}(\kappa_c)}{\bar{\sigma}(\kappa_t)}(1-\alpha) - (1+\alpha) & \text{for } (\hat{\bar{\sigma}}_1) > 0 \\ \gamma & \text{for } (\hat{\bar{\sigma}}_1) \leq 0 \end{cases}$$

$c_c(\boldsymbol{\kappa}) = \bar{\sigma}_c(\boldsymbol{\kappa}) = f_c'$ - material cohesion.

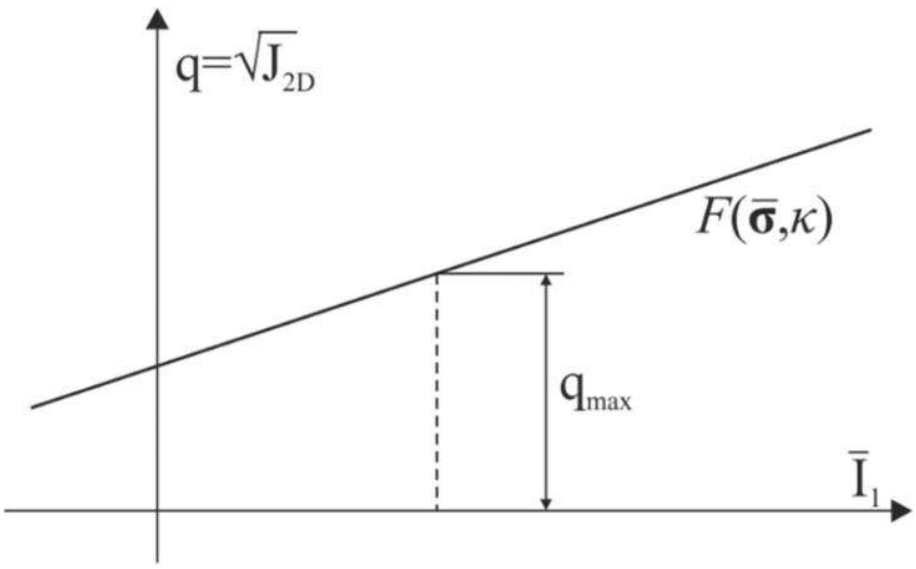

Figure 1. The failure surface of CDP model.

The parameter γ is calculated as the ratio of stress deviators in the compressive meridian (cm) and tensile meridian (tm), according to the following expression:

$$\gamma = \frac{3(1-\rho)}{2\rho - 1}$$

where $\rho = \frac{q_{tm}}{q_{cm}} = \frac{\sqrt{3J_{2D,tm}}}{\sqrt{3J_{2D,cm}}}$.

The nominal stress $\boldsymbol{\sigma}$ and the effective stress $\bar{\boldsymbol{\sigma}}$ are related by the degradation parameter d (Lubliner et al., 1989), according to:

$$\boldsymbol{\sigma} = (1-d)\bar{\boldsymbol{\sigma}} \tag{2}$$

The elastic stiffness matrix $\mathbf{D}$ is related to initial elastic stiffness matrix $\mathbf{D}_0$ by the degradation as follows (Lee, 1996):

$$\mathbf{D} = (1-d)\mathbf{D}_0 \tag{3}$$

The degradation d is a function of the damage variable $\boldsymbol{\kappa}$ and is calculated as:

$$d = 1 - (1 - d_c(\boldsymbol{\kappa}))(1 - sd_t(\boldsymbol{\kappa})) \tag{4}$$

where $d_c(\boldsymbol{\kappa})$ and $d_t(\boldsymbol{\kappa})$ represent degradations under compressive and tensile loading:

$$d_{c/t} = 1 - \left[\left(\frac{1}{a_{c/t}}\right)\left(1 + a_{c/t} - \sqrt{\phi(\kappa_{c/t})}\right)\right]^{\frac{c_{c/t}}{b_{c/t}}} \tag{5}$$

quantities $a_{c/t},\ b_{c/t}, c_{c/t}$ represents material parameters and function $\phi(\kappa_{c/t})$ is calculated as:

$$\phi(\kappa_{c/t}) = 1 + a_{c/t}(2 + a_{c/t})\kappa_{c/t} \tag{6}$$

The damage variable $\boldsymbol{\kappa}$ is defined by two independent variables κ_c and κ_t for compression and tension:

$$\boldsymbol{\kappa} = \begin{bmatrix} \kappa_t & \kappa_c \end{bmatrix} \tag{7}$$

which are calculated according to the following relations (Lee and Fenves, 1998):

$$k_{c/t} = \frac{1}{g_{c/t}} \int_o^{\varepsilon^p} \sigma_{c/t} \mathrm{d}\varepsilon^p \tag{8}$$

In expression (8), $d\varepsilon^p$ is increment of the plastic strain, while the quantities $g_{c/t}$ represents the dissipated energy density during the entire process of microcracking under uniaxial

compression and uniaxial tension respectively, and they are calculated according to the following expression:

$$g_{c/t} = \int_o^{\infty} \sigma_{c/t} \mathrm{d}\varepsilon^p \tag{9}$$

In other words, the quantities g_c and g_t represent the area under the $\sigma - \varepsilon^P$ curve for the uniaxial compression test and the uniaxial tension test, respectively. These quantities can be calculated based on the compressive and tensile fracture energy $G_{c/t}$, which represent material parameters and characteristic length (l_{ch}), according to:

$$g_{c/t} = \frac{G_{c/t}}{l_{ch}} \tag{10}$$

All those equations presented in this section are implemented into the FEM software PAK as the implicit stress integration algorithm at the integration point level. More details regarding the implementation are available in the literature (Rakić et al., 2019, 2021; Water institute Jaroslav Cerni and Faculty of Engineering, University of Kragujevac, 2017).

Strength reduction method for CDP model

For the geotechnical constitutive models without damage, the SRM is implemented by gradually reducing the strength of the material and reducing the failure surface, which brings the analyzed structure to the state of limit equilibrium. However, for the constitutive models which include damage feature, such as the CDP model, it is necessary to reduce the failure surface in the meridional plane, which means that the parameters for failure surface definition, and the ratio of uniaxial and biaxial stress at failure will be reduced. In this way, in addition to the size, also the shape of the failure surface in the deviatoric plane would change, which changes the character of the material's behavior, which is the undesired effect (Figure 2).

As the possible solution for reducing the strength of the material for the CDP model, without changing the shape of the failure surface, it is necessary to modify the dependence that describes the

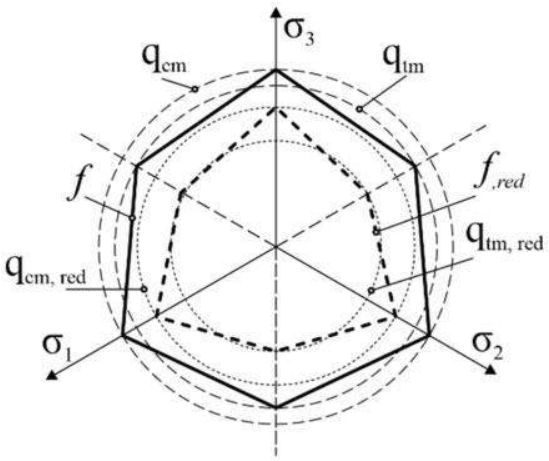

Figure 2. Undesirable change of the shape of the failure surface in the deviatoric plane.

material's behavior in uniaxial compression and uniaxial tension tests. In other words, it is required to reduce the parameters for the material's behavior definition in the uniaxial compression and uniaxial tension tests, as shown in Figure 3.

To achieve desired material behavior, it is necessary to modify the stress-plastic strain relation (Figure 3(a) and (b)) by reducing the uniaxial compressive strength f_c' and uniaxial tensile strength f_t':

$$f'_{c/t,red} = \frac{f_{c/t}}{SRF} \tag{11}$$

To reduce the area under the curve $\sigma - \varepsilon^P$, as defined by the expression (9), it is necessary to the reduce the compressive fracture energy G_c and the tensile fracture energy G_t:

$$G_{c/t,red} = \frac{G_{c/t}}{SRF^2} \tag{12}$$

As the quantitates g_c and g_t represent the area under the stress-plastic strain curves, in order to reduce stress as well as the plastic strain, this energy needs to be reduced by the square of SRF, as shown in equation (12) and graphically interpreted in Figure 3. The relationship between dissipated energy density and fracture energy is defined by the following expression (Lee and Fenves, 1998):

$$g_{c/t,red} = \frac{G_{c/t,red}}{l_{ch}} \tag{13}$$

therefore, reducing the fracture energy $G_{c/t}$ reduces the dissipated energy density $g_{c/t}$, which results in an increased value of damage variable $k_{c/t}$:

$$k_{c/t,red} = \frac{1}{g_{c/t,red}} \int_o^{\varepsilon^p} \sigma_{c/t} \mathrm{d}\varepsilon^p \tag{14}$$

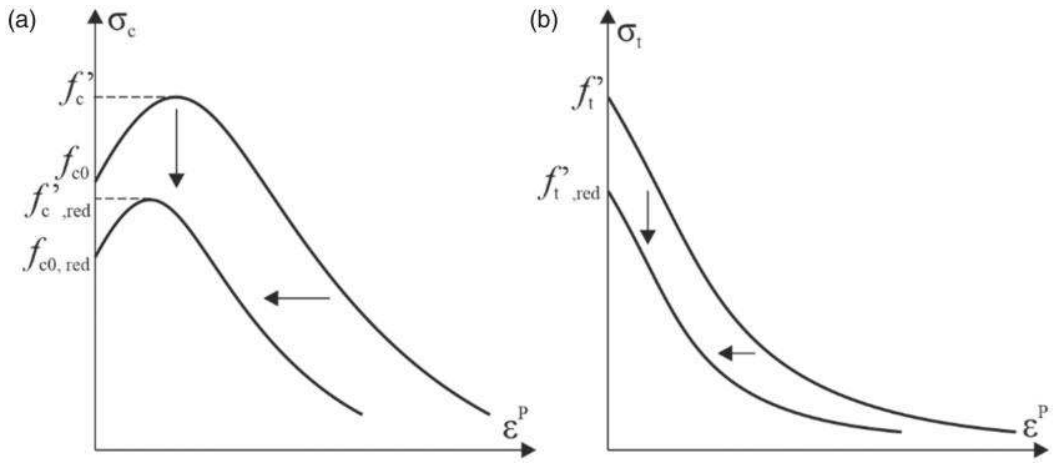

Figure 3. Strength reduction in uniaxial (a) compression and (b) tension.

By increasing the damage variable $k_{c/t}$, the function $\phi(\kappa_{c/t,red})$ also increases:

$$\phi(\kappa_{c/t,red}) = 1 + a_{c/t}(2 + a_{c/t})\kappa_{c/t,red} \tag{15}$$

which causes an increase in the material degradation according to (5), which reduces the elastic stiffness matrix in accordance with (3) and reduces strength of material, which was the goal of the proposed procedure.

Numerical implementation of SRM for CDP model

The proposed procedure for determining the FoS by SRM using the CDP model, is further prepared as a numerical algorithm shown in Figure 4. The algorithm is implemented as a wrapper for the software PAK, which controls the execution and calculates the FoS for the desired structures. The complete FE analysis of the structure is performed, for each algorithm iteration. The wrapper controls the computed values of SRF and calculates the FoS. In the presented algorithm of the SRM, X_a represents the left (lower) boundary of the FoS (for which there is a convergence of numerical solutions), while X_b is the right (upper) boundary of the FoS (for which there is no convergence of numerical solutions).

The initial boundaries represent the two values of SRF between which the solution for FoS is located. To determine the initial boundary values for the bisection method, it is possible to use any of the known numerical techniques (Kojić and Bathe, 2005). As the left boundary X_a represents the value of the SRF for which there is a convergence of numerical solutions, while the right boundary X_b represents the value of the SRF for which there is no convergence of numerical solutions. It is possible, for example, to adopt the initial value of the left boundary $X_a = 1$, and to calculate the

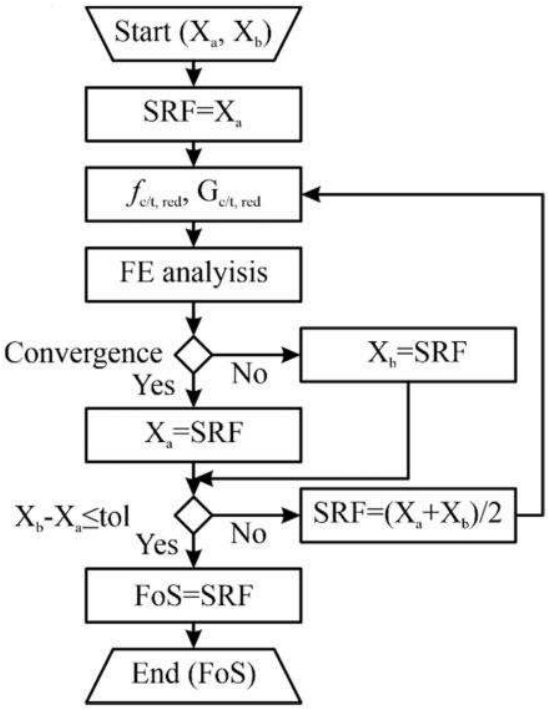

Figure 4. Block diagram for SRM implementation using CDP model.

right boundary as $X_b = 2*X_a$. If there is convergence of the numerical solutions for both the values X_a and X_b, the initial boundaries should be corrected so that the left boundary becomes $X_a = X_b$, while the right boundary increases according to $X_b = 2*X_a$ until there is no convergence of the numerical solution. After determining the boundary values, the FoS is determined between them using the bisection method previously described in the Figure 4.

Numerical examples

To verify the proposed procedure, several numerical analyses were carried out. Other analytical or numerical safety assessment methods do not consider the presented verification examples in the literature. Therefore, the theoretical values of FoS are calculated based on FoS analytical definition for the simple uniaxial loading examples to show that obtained numerically computed FoS values are correct.

The verification examples are uniaxial compression test, uniaxial tension test, and bending test of the concrete beam without reinforcement. The first simulation was conducted using applied stress and the FoS was determined. To analyze the post-critical behavior (behavior after overcoming the peak strength) and to verify the proposed methodology on the entire range of strain, the second simulations were realized by using the prescribed displacements. The constitutive model parameters used in the numerical simulations were obtained by material parameters identification. They are adopted from the report on the stability analysis of the concrete arch dam (Water institute Jaroslav Cerni, 2019). The used material parameters are shown in Table 1.

The proposed examples are created to show accuracy and functionality of the SRM. Due to the lack of verification examples from literature, the only possibility was to create the examples, which can be solved analytically also. In the case of the problems where the structure response cannot be predicted, the analytical value of the load cannot be determined, and the only possibility is the proposed SRM.

Uniaxial compression and tension test

The FE model used for the numerical simulation of the uniaxial compression test and the uniaxial tension tests consists of one eight-node 3 D finite element of unit dimensions. The model has three planes of symmetry, so one-eighth of the model was modeled using the appropriate boundary conditions. The layout of the FE model with the boundary conditions and the loads for the uniaxial compression and the tension tests are shown in Figure 6(a), while the load function is shown in Figure 6(b).

To obtain the FoS in the uniaxial compression test, in the first simulation the model was loaded by applying compression stress, while in the uniaxial tensile test, the load of the model was applied using tension stress on the upper side of the model. The boundary conditions and the loads for the compression and tension tests are shown in Figure 5(a), while the load function is shown in Figure 5(b). In both tests, the loads were applied using 100 equal-time increments and increased linearly up to the maximum value. The two stress values were chosen for FoS calculation in the

Table 1. Material parameters of CDP constitutive model in the numerical examples.

E [GPa]	ν [−]	f_c' [MPa]	f_t' [MPa]	G_c [kN/m]	G_t [kN/m]	α [−]	α_p [−]	s_0 [−]	D_c [−]	D_t [−]	a_c [−]	a_t [−]	γ [−]
26.48	0.184	32.4	1.78	95.6	2.4	0.12	0.26	0.0	0.35	0.655	3.074	0.75	3.0

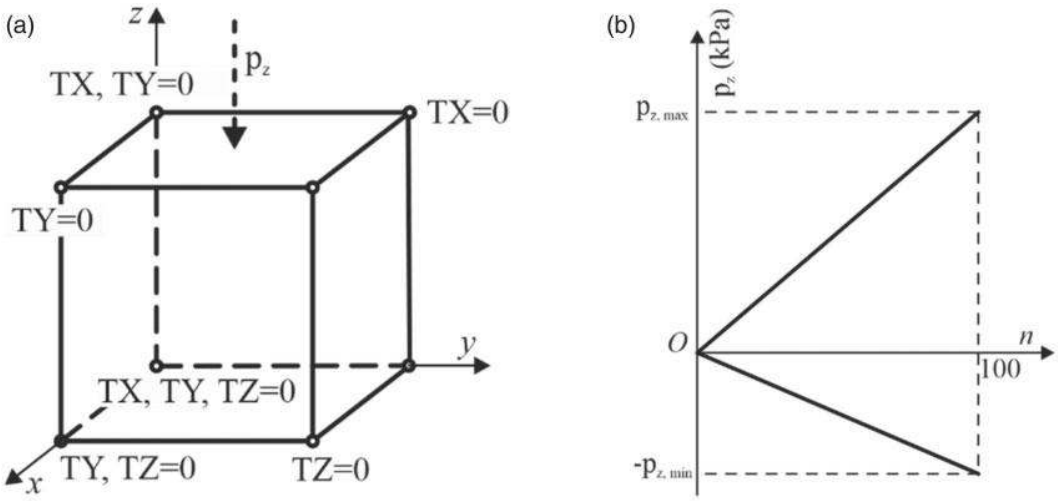

Figure 5. Uniaxial compression and tension test using prescribed pressure a) FE model, b) load functions.

uniaxial compression tests: 10 MPa and 20 MPa, while for the tension test, the FoS was calculated for two levels of tensile stress: 0.75 MPa and 1.5 MPa.

In order to compare the results, the FoS can also be calculated analytically, which is usually not possible in the case of complex stress states. In this case, the analytical FoS is calculated as the ratio of the uniaxial strength of the material and the applied stress value:

$$FOS_{theory} = \frac{f'_{c/t}}{\sigma_{c/t}} \tag{16}$$

Applying the SRM procedure, the FoS for defined loads are numerically calculated. The FoS obtained analytically and numerically are compared and the values are shown in Table 2 in the case of compression test and Table 3 in the case of tension test.

In the second numerical simulation the models were loaded using prescribed displacements at the nodes on the upper surface of the model, in order to ensure numerical convergence over the entire strain range. The load was applied using $n = 100$ equal time steps and linearly increased up to the maximum value of the prescribed displacement, which in the case of compression test was 0.01, while in the case of tension test was 0.005 (Figure 6(b)). Since the FE model of unit dimensions was used, the displacement corresponds to the total strain and in the case of the compression test was $\varepsilon = 0.01$, while in the case of the tension test, the total strain was $\varepsilon = 0.005$.

The simulation results are shown in Figures 7 and 8 for compression and Figures 9 and 10 for the tension test in the form of the dependence of the normal stress to the total strain and the plastic strain, as well as the normal stress and the plastic strain as a function of degradation for the different values of the SRF.

The charts given in Figures 7 and 9 show the impact of the reduction of the fracture energy, where it can be seen that in addition to the stress, the total strain and plastic strain were reduced. The straight lines in Figures 7(a) and 9(a) show the analytical values of stress and total strain obtained by reducing the nominal value of the uniaxial stress by the specified SRF and the corresponding strain.

The effect of applying the SRM on the failure surface for SRF values corresponding to the theoretical FoS obtained in the uniaxial compression test, according to (1), is shown in Figure 11.

Table 2. FoS for the uniaxial compression test.

σ_c (MPa)	f_c' (MPa)	$FoS_{\_theory}$	$FoS_{\_simulation}$
10	32.4	3.24	3.22
20	32.4	1.62	1.61

Table 3. FoS for the uniaxial tension test.

σ_t (MPa)	f_t' (MPa)	$FoS_{\_theory}$	$FoS_{\_simulation}$
0.75	1.78	2.37	2.37
1.50	1.78	1.18	1.18

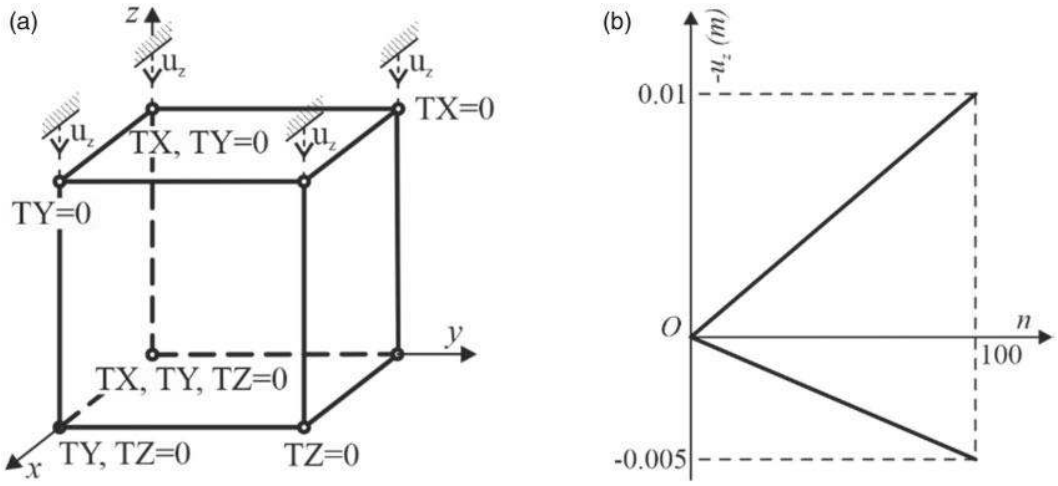

Figure 6. Uniaxial compression and tension test using prescribed displacement (a) FE model and (b) load functions.

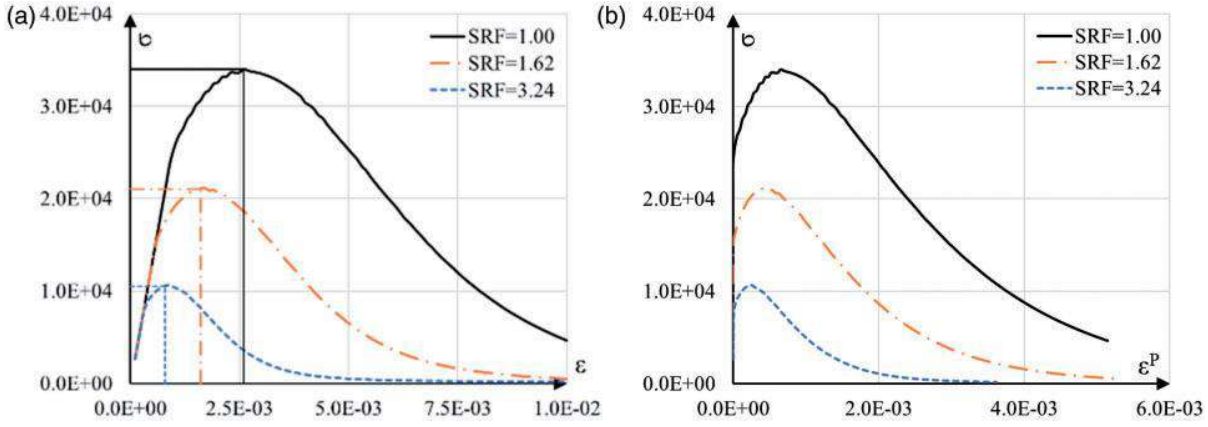

Figure 7. Normal stress as a function of (a) total strain and (b) plastic strain in compression test.

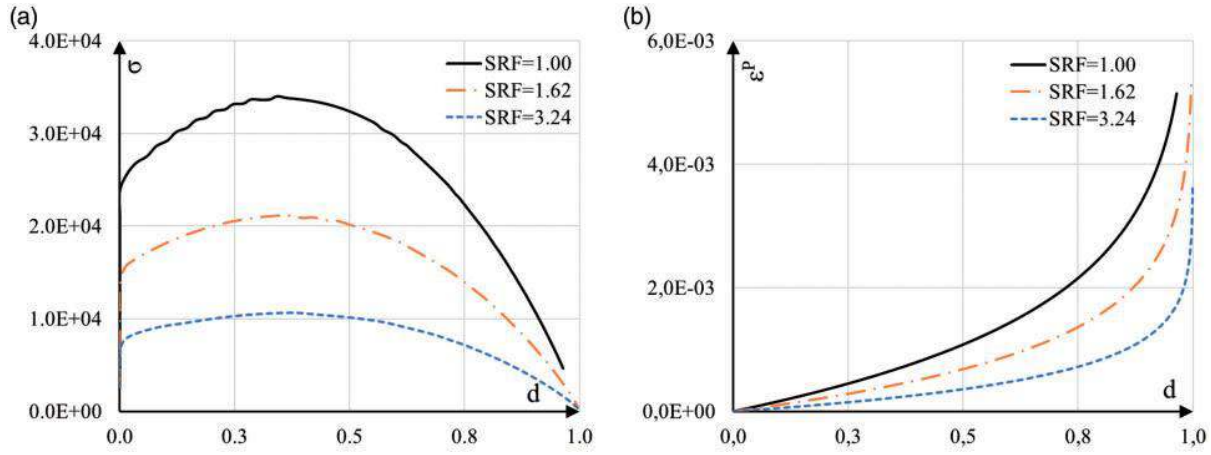

Figure 8. Dependence of (a) stress and (b) plastic strain on degradation in compression test.

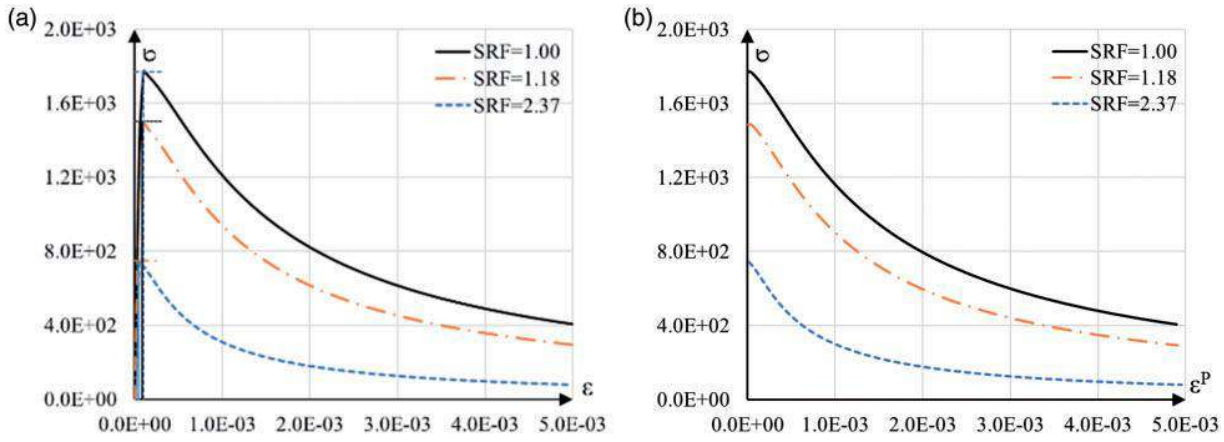

Figure 9. Normal stress as a function of (a) total strain and (b) plastic strain in tension test.

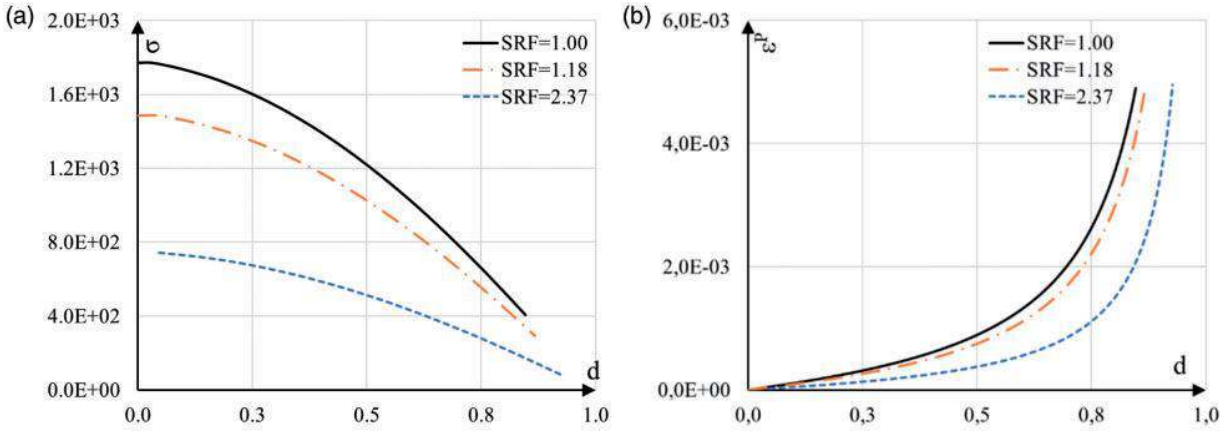

Figure 10. Dependence of (a) stress and (b) plastic strain on degradation in tension test.

The figure also shows stress paths in the entire load range (dashed lines): from zero to the maximum value of the applied pressure. From this figure it can be seen that the failure surface is reduced by the given SRF value and that the failure in the material occurs when the stress point reaches the reduced failure surface.

Based on the obtained results, it can be concluded that the stress and the related total strain were reduced for the prescribed value of the SRF in the entire range of strain. The original uniaxial numerical examples are simulated according to original CDP constitutive model developed by (Lee, 1996). As it can be noticed, the stress-strain curves are reduced by increasing of SRF (FoS = SRF see Figure 4), because of material strength is decreased, what means that for the higher FoS, we consider the material as a weaker one (Figures 7 and 9).

By comparing the values shown in Table 2 and Figure 7(a) for the compression test and Table 3 and Figure 9(a) for the tension test, it can be concluded that by applying the proposed SRM procedure for the CDP model, the obtained FoS correspond to the analytical FoS.

Four points bending of concrete girder

The following example shows the FoS determination in the case of concrete girder bending (Šumarac et al., 2003). The layout of the FE model, dimensions, boundary conditions and loads are shown in Figure 12. Dimensions in the figure are given in mm.

To determine the maximum force required to bend the concrete girder, the first simulation was carried out by using the prescribed displacements. The material parameters used in this numerical simulation of the concrete girder bending test are the same as in the previous examples and are shown in Table 1.

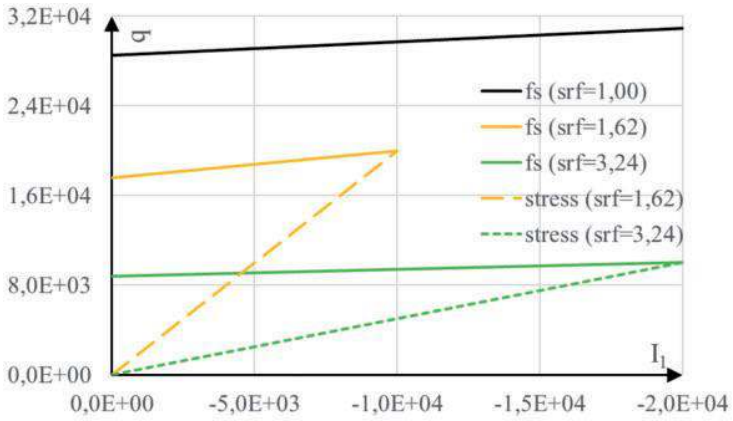

Figure 11. Reduced failure surface and corresponding stress paths.

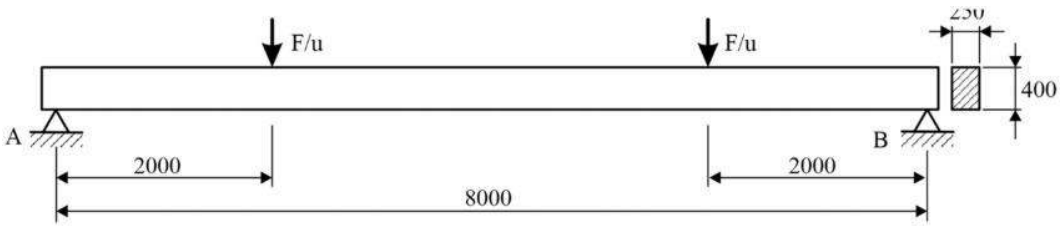

Figure 12. Bending of concrete girder.

After the simulation using prescribed displacement, the obtained results are shown in Figure 13 as a dependence of the force vs. prescribed displacement. The horizontal dashed line in Figure 13 represents the maximum value of the force for girder bending.

The maximum computed force is used to calculate the theoretical FoS of the concrete girder, in order to compare it with the numerical solution for FoS, according to the following expression:

$$FoS_{theory} = \frac{F_{\max}}{F} \tag{17}$$

In the second simulation, the determination of the FoS of the concrete girder was carried out by using the SRM, where the girder is loaded using the prescribed force. Two force values of lower intensity than the maximum force, determined by applying the specified displacements, are used to determine the FoS. The analytical and the numerical FoS values of the bending test are shown in Table 4.

To analyze the dependence of the bending force on the displacement in the entire range of strain, the third simulation was carried out using the prescribed displacement, whereby the material strength was reduced using values of SRF corresponding to the theoretical FoS (SFR = FoS) from Table 4. The results of this simulation are shown in Figure 14. The dashed lines show the values of the forces obtained by reducing the strength of material from the first test using the analytical values of the SRF = FoS from Table 4.

By comparing the FoS obtained analytically to the FoS obtained by applying the SRM, it can be concluded that the calculated values using the two different approaches are very close.

The fields of axial stress, plastic strain, and material degradation of the girder at the end of loading process are shown in Figures 15 to 17 for the case of a nominal strength of the material (SRF = 1.00), as well as for the case of reduced material strength (SRF = 1.65 and SRF = 2.64).

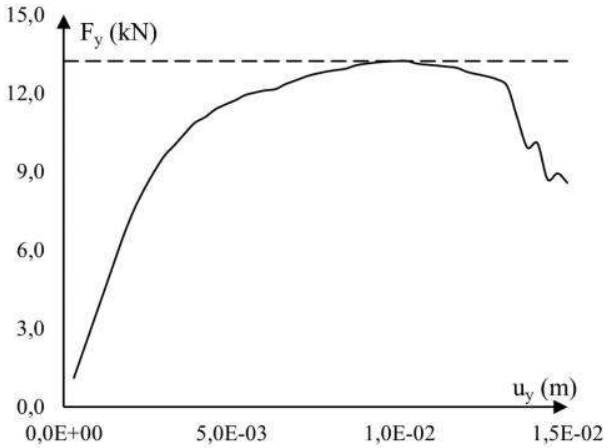

Figure 13. Computed bending force vs. displacement for nominal material parameters.

Table 4. The FoS of beam in bending test.

F (kN)	$F_{,max}$ (kN)	FoS_{theory}	$FoS\_{simulation}$
5.0	13.22	2.64	2.68
8.0	13.22	1.65	1.68

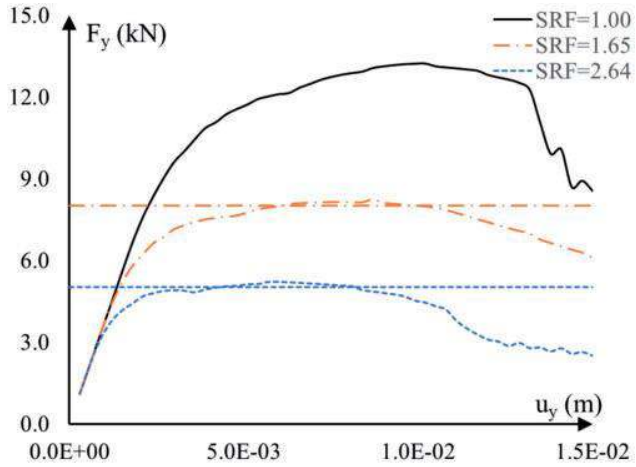

Figure 14. Bending force vs. displacement for reduced material parameters.

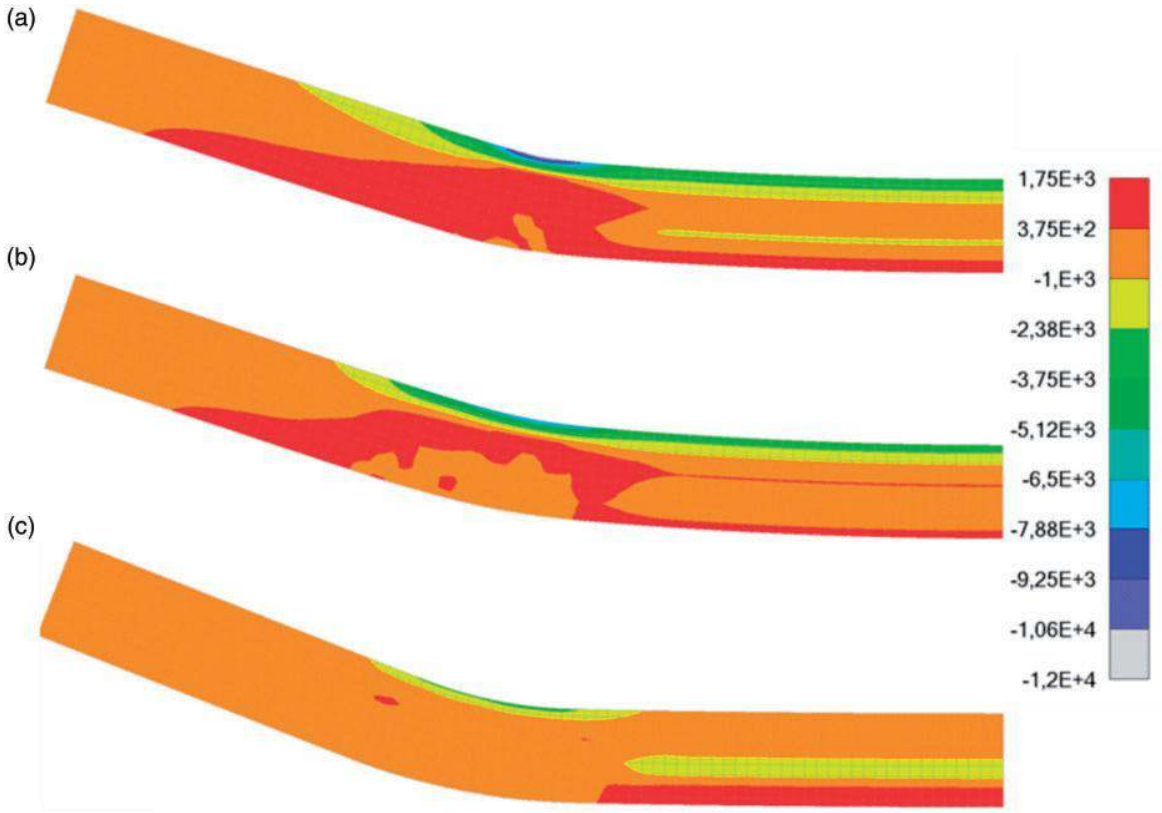

Figure 15. Axial normal stress: (a) SRF = 1.00; (b) SRF = 1.65 and (c) SRF = 2.64.

As it can be noticed from the block diagram in Figure 4, the determined FoS is equal to the value of SRF in the final iteration, so the material properties are reduced by the SRF = FoS. The simulation results of the structure with the reduced strength of the material, show the state of limit equilibrium (the state immediately before the failure) for the same prescribed loading conditions. The consequences are the decreased maximal stresses in the structure, and the increased level of plastic strain and degradation, because of the reduced strength of the material.

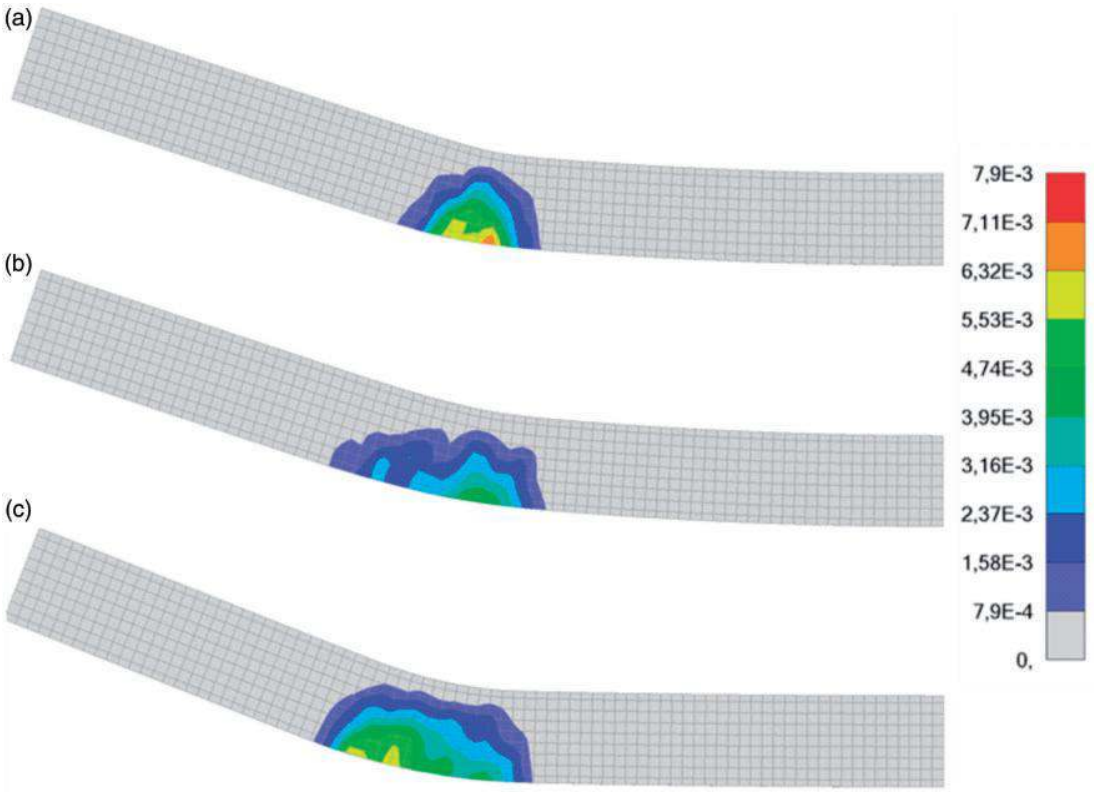

Figure 16. Equivalent plastic strain: a) SRF = 1.00; b) SRF = 1.65; c) SRF = 2.64.

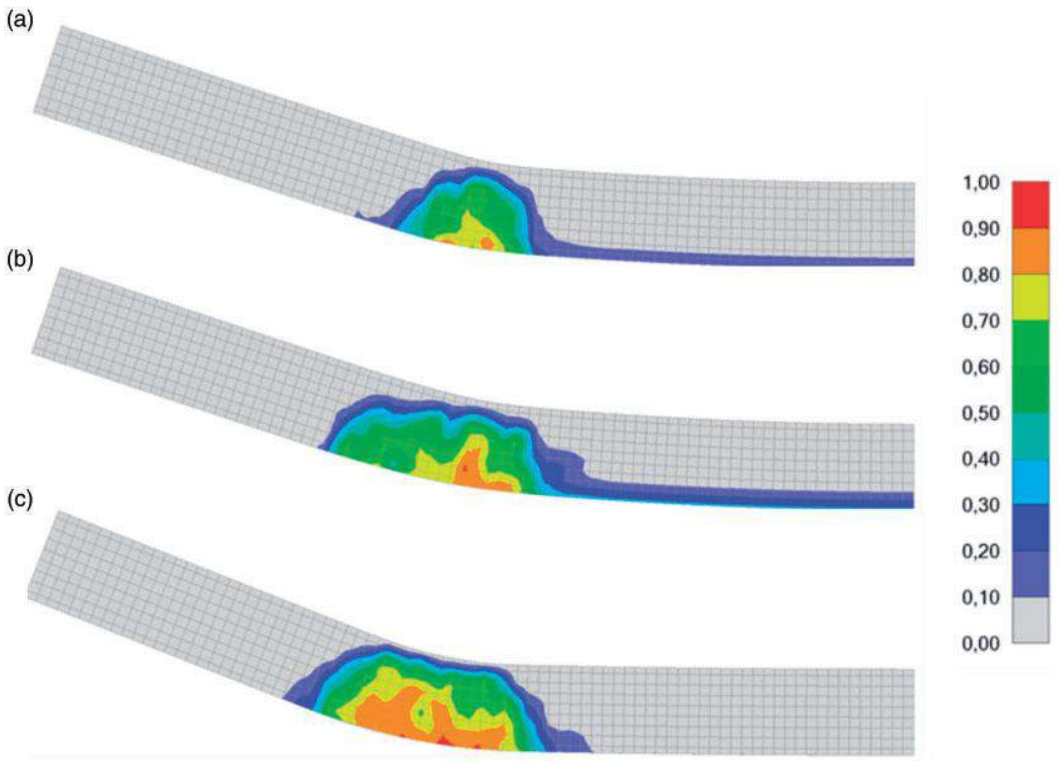

Figure 17. Degradation: (a) SRF = 1.00; (b) SRF = 1.65 and (c) SRF = 2.64.

In Figure 15, it can be seen that with an increase in SRF, the normal stress in the cross-section decreases, which is a consequence of the reduction of the strength of the material. However, at the same time, there is an increase in plastic strain, which occurs in the wider area under the place of applied load, which can be seen in Figure 16.

With an increase in the strength reduction factor, there is an increase of the material degradation, which occurs in the wider area below the place of application of the load (Figure 17).

The presented analysis results show that the proposed procedure for determining of FoS for the CDP constitutive model gives FoS very close to the analytical values. Hence, the proposed procedure is accurate enough for practical application in the safety analysis of real concrete structures.

Conclusions

Reducing material strength using the procedure of reducing the failure surface can be used to determine the global FoS for constitutive models without damage feature. However, this approach cannot be used in the strength reduction for constitutive models with the damage feature. The main reason is that when reducing the failure surface using the SRF, the shape of this surface changes in the deviator plane, which changes the description of the behavior of the material. Nevertheless, the SRM for determining the global FoS can be successfully applied to the CDP model with certain modifications of the proposed procedure. The reduction of the constitutive model parameters that correspond to the reduced stress-strain description in the uniaxial compression and the uniaxial tension tests is necessary. For the proposed strength reduction procedure in the case of application to the concrete damage plasticity constitutive model, a numerical algorithm was developed and implemented in the PAK software. The developed algorithm was verified through the test examples. The numerical simulations of the uniaxial compression test, the uniaxial tension test, and the bending test of a concrete girder without reinforcement show an excellent agreement between the obtained FoS using SRM and analytically obtained FoS. Based on the above, the developed methodology can be applied to determine the global FoS of real concrete structures.

Declaration of conflicting interests

The author(s) declared no potential conflicts of interest with respect to the research, authorship, and/or publication of this article.

Funding

The author(s) disclosed receipt of the following financial support for the research, authorship, and/or publication of this article: This research is partly supported by the Ministry of Education, Science and Tecnological Development, Republic of Serbia, Grant TR32036 and Grant TR37013.

ORCID iDs

Dragan Rakić https://orcid.org/0000-0001-5152-5788
Vladimir Dunić https://orcid.org/0000-0003-1648-1745

References

Abra O and Ben Ftima M (2020) Development of a new design approach of reinforced concrete structures based on strength reduction method. *Engineering Structures* 207: 110192.

Bentley Systems International Limited (2019) *Plaxis 2D Reference Manual*. Dublin: Bentley Systems International Limited.

Bishop A W (1955) The use of the slip circle in the stability analysis of slopes. *Géotechnique* 5(1): 7–17.

Caspeele R, Sykora M, Lorenzo Allaix D, et al. (2013) The design value method and adjusted partial factor approach for existing structures. *Structural Engineering International* 23(4): 386–393.
Cheng Y, Lansivaara T and Wei W (2007) Two-dimensional slope stability analysis by limit equilibrium and strength reduction methods. *Computers and Geotechnics* 34(3): 137–150.
Couto D, Carvalho M, Cintra A, et al. (2015) Concrete structures. Contribution to the safety assessment of existing structures. *Revista Ibracon De Estruturas E Materiais* 8(3): 365–389.
Dawson E and Roth W (1999) Slope stability analysis by strength. *Géotechnique* 49(6): 835–840.
Fu W and Liao Y (2010) Non-linear shear strength reduction technique in slope stability calculation. *Computers and Geotechnics* 37(3): 288–298.
Griffiths D V and Lane P A (1999) Slope stability analysis by finite elements. *Géotechnique* 49(3): 387–403.
Hammah R, Yacoub T and Corkum B (2005) *The Shear Strength Reduction Method for the Generalized Hoek-Brown Criterion*. Alaska, s.n: Anchorage.
Janbu N (1954) *Application of Composite Slip Surface for Stability Analysis*. In: *Proceedings of European Conference on Stability of Earth Slopes*, Sweden, pp. 43–49.
Kiefer B, Waffenschmidt T, Sprave L, et al. (2018) A gradient-enhanced damage model coupled to plasticity – multi-surface formulation and algorithmic concepts. *International Journal of Damage Mechanics* 27(2): 253–295.
Kojić M and Bathe K-J (2005) *Inelastic Analysis of Solids and Structures*. Berlin: Springer.
Kojić MI and Drugi (2010) *Software for geomechanics – PAK-GEO*., Kragujevac: Faculty of Mechanical Engineering, University of Kragujevac.
Kojić M, Slavković R, Živković M, et al. (2011), *PAK-S: Program for FE Structural Analysis*., Kragujevac: University of Kragujevac, Faculty of Engineering.
Lara C, Tanner P, Zanuy C, et al. (2021) Reliability verification of existing RC structures using partial factors approaches and site-specific data. *Applied Sciences* 11(4): 1653.
Lee J (1996) *Theory and Implementation of Plastic-Damage Model for Concrete Structures under Cyclic and Dynamic Loading*., Berkeley: University of California.
Lee J and Fenves G (1998) Plastic-damage model for cyclic loading of concrete structures. *Journal of Engineering Mechanics* 124(8): 892–900.
Li L, Tang C, Zhu W, et al. (2009) Numerical analysis of slope stability based on the gravity increase method. *Computers and Geotechnics* 36(7): 1246–1258.
Lubliner J, Oliver J, Oller S, et al. (1989) A plastic-damage model for concrete. *International Journal of Solids and Structures* 25(3): 299–326.
Manzari M T and Nour M A (2000) Significance of soil dilatancy in slope stability analysis. *Journal of Geotechnical and Geoenvironmental Engineering* 126(1): 75–80.
Naylor DJ (1982) Finite elements and slope stability. In: JB Martins (ed) *Numerical Methods in Geomechanics*. NATO Advanced Study Institutes Series, vol 92. Springer, Dordrecht. https://doi.org/10.1007/978-94-009-7895-9_10
Omidi O and Lotfi V (2010) Finite element analysis of concrete structures using plastic-damage model in 3-D implementation. *International Journal of Civil Engineering* 8(3): 187–203.
Park T, Ahmed B and Voyiadjis G Z (2022) A review of continuum damage and plasticity in concrete: Part I – Theoretical framework. *International Journal of Damage Mechanics* 31(6): 901–954.
Rakić D M, Bodić A S, Milivojević N J, et al. (2021) Concrete damage plasticity material model parameters identification. *Journal of the Serbian Society for Computational Mechanics* 15(2): 111–122.
Rakić D, Dunić V, Živković M, et al. (2019) Modeling of damaged concrete using initial degradation parameter. *Journal of the Serbian Society for Computational Mechanics* 13(2): 8–18.
Sarma S K (1973) Stability analysis of embankments and slopes. *Géotechnique* 23(3): 423–433.
Seo Y K (1998) *Computational Methods for Elastoplastic Slope Stability Analysis with Seepage*. USA: The University of Iowa.
Spencer E (1967) A method of analysis of the stability of embankments assuming parallel inter-slice forces. *Géotechnique* 17(1): 11–26.

Šumarac D, Sekulović M and Krajčinović D (2003) Fracture of reinforced concrete beams subjected to three point bending. *International Journal of Damage Mechanics* 12(1): 31–44.

Voyiadjis G Z, Ahmed B and Park T (2022) A review of continuum damage and plasticity in concrete: Part II – Numerical framework. *International Journal of Damage Mechanics* 31(5): 762–794.

Water institute Jaroslav Cerni (2019), *Dam Safety Management System: Report on Analyzes Using FE Models of Thermal, Filtration and Stress-Strain Processes*. Belgrade: Water institute Jaroslav Cerni.

Water institute Jaroslav Cerni and Faculty of Engineering, University of Kragujevac (2017) *Algorithm and Implementation of the Stress Integration Procedure for the Concrete Material Model with Damage, Verification Examples and Description of the Structure of the Input File for the PAK Program*. Belgrade: Water institute Jaroslav Cerni.

Woliński S (2011) Global safety factor for nonlinear design of concrete structures. *Archives Of Civil Engineering* LVII(3): 331–339.

Xue H, Dang F, Yin X, et al. (2018) Unified overload method of slope stability analysis based on potential sliding direction. *KSCE Journal of Civil Engineering* 22(9): 3254–3262.

Zhang P W and Chen Z Y (2004) Finite element method for solving safety factor of slope stabilily. *Rock and Soil Mechanics* 25(11): 1757–1760.

Zhao S and Zheng Y (2002) *Slope Safety Factor Analysis Using ANSYS*. China: Logistical Engineering University, ChongQing.

Zheng H, Sun G and Liu D (2009) A practical procedure for searching critical slip surfaces of slopes based on the strength reduction technique. *Computers and Geotechnics* 36(1–2): 1–5.

Zienkiewicz O, Humpheson C and Lewis R (1975) Associated and nonassociated viscoplasticity in soil mechanics. *Géotechnique* 25(4): 671–689.